Motion of damped Langmuir solitons in inhomogeneous plasmas

S. Bujarbarua
Department of Physics, Dibrugarh University, Dibrugarh-786004, India

E. W. Laedke and K. H. Spatschek
Fachbereich Physik, Universität Essen, D-4300 Essen, Federal Republic of Germany
(Received 1 December 1981)

The dynamics of envelope solitons accompanied by density depressions (cavitons) is analyzed with the use of the driven Zakharov equations for inhomogeneous plasmas; damping effects are included. The acceleration in a spatially inhomogeneous plasma is found to be dominated by ion inertia, in contrast to the corresponding (adiabatic) Schrödinger predictions. The maximum speed is the ion-sound velocity. The dynamic-plasma response hinders the center of the wave packet from obeying a Newtonian force equation with the inhomogeneity acting as a force. Damping terms in the high-frequency equation introduce a new acceleration mechanism which is investigated explicitly. We analyze these effects on the basis of a moment method which starts from conservation laws. Finally, the complete set of equations, in the presence of a driver, is solved numerically. Energy transfer and relaxation oscillations are investigated.

I. INTRODUCTION

Since the discovery of the soliton many papers dealt with the mathematical and physical aspects of integrable systems. Later on, to cover more realistic physical situations, a singular perturbation theory was developed[1,2] to describe the long-time cumulative effects of weak perturbations on solitons. For example, it was shown how the nonlinear Schrödinger soliton can become synchronized to a periodic external field and how it moves in gradual field gradients.

In plasma physics, instead of the nonlinear Schrödinger equation the so-called Zakharov equations[3] are often the proper nonlinear equations. The Zakharov equations consist of an averaged high-frequency equation which describes, e.g., the envelope of an Langmuir field and a coupled equation for the (linearized) plasma response in the presence of the ponderomotive force of the Langmuir wave. No inverse scattering transform exists for the Zakharov equations. Therefore one might think of treating the dynamic-plasma response as a perturbation on a nonlinear Schrödinger equation in order to apply the well-developed perturbation technique. There are no objections against such a treatment as long as the dynamical effects are small. If one wants to study the motion of perturbed Zakharov solitons, e.g., the effect of spatial inhomogeneity, such perturbational calculations would treat the inhomogeneity (and, in addition the external field, damping, etc.) on the same footing as the dynamic-plasma response. However, a perturbation theory on the fully developed Zakharov soliton would be more desirable in many physical applications.

Therefore, in the past, mathematically less-rigorous but physically more-plausible methods have been proposed[4–11] to investigate the motion of perturbed solitons when the zeroth-order equations are nonintegrable. One commonly used treatment consists of approximate solutions of the balance equations. We shall apply this moment method here.

We want to investigate the motion of Zakharov solitons in the presence of spatial inhomogeneity, damping, and a driver. Physically such an investigation is motivated by many applications. We mention only the mode-converted localized electron plasma wave at the critical density.[5,7,11] The low-frequency ponderomotive force of the Langmuir wave drives the plasma, locally creating a density cavity. Depletion of the local plasma density allows the cavity to trap the high-frequency fields. The cavity carrying the local electric field then propagates out from the resonant region in an inhomogeneous plasma. It is still influenced by the incoming radiation; this coupling is usually modeled by a constant driver. When the amplitude of the soliton increases because of energy transfer from the driver, its width is expected to shrink and Landau damping might become important.

This type of problem was recently considered

analytically.[5,7,9,11] Chen and Liu[5] presented results for soliton generation within the static approximation. Then the soliton can be strongly accelerated down a density gradient. This acceleration will be reduced by ion inertia.[9,11] One purpose of this paper is to demonstrate this effect in more detail. In addition we want to investigate the effect of damping[12–14] on the motion of the soliton. In the case of the nonlinear Schrödinger equation, no essential new effects are expected. However, for the Zakharov equations the situation is different as has been first pointed out by Chukbar and Yankov.[6] A damping of the high-frequency wave can lead to acceleration of the soliton.

The plan of the paper is as follows. In Sec. II we derive the basic balance equations and the corresponding ordinary differential equations for the soliton parameters. In Sec. III we study the *undriven* Zakharov equations in an inhomogeneous plasma in the presence of damping. The undamped inhomogeneous case is solved analytically. The results are compared with previous predictions. Next, the acceleration because of damping is demonstrated. In Sec. IV we allow for a driver. Analytical estimates and numerical results for the *driven* inhomogeneous case with Landau damping are presented. The paper is concluded by a short summary and outlook in Sec. V.

II. BASIC EQUATIONS

We describe the evolution of the electric field E by a nonlinear Schrödinger equation in which the density modification δn is governed by the ion-acoustic wave equation with the effects of the ponderomotive force included self-consistently. In the one-dimensional electrostatic approximation and for small driving fields E_d, the basic equations are[3]

$$2i\frac{\partial E}{\partial t}+3\omega_{\rm pe}\lambda_e^2\frac{\partial^2 E}{\partial x^2}-\omega_{\rm pe}\left[\frac{\delta n}{n_0}+\frac{x}{L}\right]E=E_d+i\Gamma E\ , \tag{1}$$

$$\frac{\partial^2\delta n}{\partial t^2}-c_s^2\frac{\partial^2\delta n}{\partial x^2}=\frac{1}{16\pi m_i}\frac{\partial^2|E|^2}{\partial x^2}\ . \tag{2}$$

Here,

$$\omega_{\rm pe}=(4\pi n_0 e^2/m_e)^{1/2}$$

is the electron plasma frequency,

$$\lambda_e=(T_e/4\pi n_0 e^2)^{1/2}$$

is the electron Debye length, L is the characteristic length of the (linear) density inhomogeneity,

$$c_s=(T_e/m_i)^{1/2}$$

is the ion-sound speed, and Γ is the damping coefficient. Introducing the units $\sqrt{3}/\omega_{\rm pi}$ and $\sqrt{3}\lambda_e$ for normalization of time and space, we find[11] for

$$E/(16\pi n_0 T_e)^{1/2}\rightarrow E\ ,$$

$\Gamma/\omega_{\rm pe}\rightarrow\Gamma$, $\delta n/n_0=n$, and $\alpha=\sqrt{3}\lambda_e/L$,

$$i\epsilon\frac{\partial E}{\partial t}+\frac{\partial^2 E}{\partial x^2}-(\alpha x+n)E=E_d+i\Gamma E\ , \tag{3}$$

$$\frac{\partial^2 n}{\partial t^2}-\frac{\partial^2 n}{\partial x^2}=\frac{\partial^2|E|^2}{\partial x^2}\ . \tag{4}$$

The parameter ϵ is given by the electron to ion mass ratio, $\epsilon=2(m_e/3m_i)^{1/2}$; ω_{pi} is the ion plasma frequency.

In order to solve Eqs. (3) and (4), we apply the approximative but powerful moment method. The following modified conservation laws are used.

For the plasmon number we get

$$i\epsilon\frac{\partial}{\partial t}\int_{-\infty}^{+\infty}EE^*dx=-E_d\int_{-\infty}^{+\infty}(E-E^*)dx-2i\Gamma\int_{-\infty}^{+\infty}EE^*dx\ , \tag{5}$$

after multiplication of Eq. (3) by E^*, adding the complex conjugate, and integration. Here and in the following we assume that all quantities are localized in space. In a similar way, we find for the total momentum

$$\frac{\partial}{\partial t}\int_{-\infty}^{+\infty}(i\epsilon EE_x^*+nu)dx=-\alpha\int_{-\infty}^{+\infty}EE^*dx-2i\Gamma\int_{-\infty}^{+\infty}E_x^*E\,dx\ , \tag{6}$$

where the velocity u is related to the density depression n by

$$\frac{\partial u}{\partial x}=-\frac{\partial n}{\partial t}\ . \tag{7}$$

The energy balance yields

$$\frac{\partial}{\partial t}\int_{-\infty}^{+\infty}(E_xE_x^*+nEE^*+\tfrac{1}{2}n^2+\tfrac{1}{2}u^2)dx$$
$$=-\alpha\frac{\partial}{\partial t}\int_{-\infty}^{+\infty}xEE^*dx-E_d\frac{\partial}{\partial t}\int_{-\infty}^{+\infty}(E+E^*)dx+i\Gamma\int_{-\infty}^{+\infty}\left[E\frac{\partial E^*}{\partial t}-E^*\frac{\partial E}{\partial t}\right]dx\ . \quad (8)$$

Eqs. (5), (6), and (8) correspond to the three exact conservation laws for the unperturbed Zakharov equations.

In addition, we use the balance equations for the center of gravity of the motion and the phase ψ. We get

$$i\epsilon\frac{\partial}{\partial t}\int_{-\infty}^{+\infty}xEE^*dx=-\int_{-\infty}^{+\infty}[2EE_x^*+xE_d(E-E^*)]dx-2i\Gamma\int_{-\infty}^{+\infty}xEE^*dx \quad (9)$$

and

$$-\epsilon\int_{-\infty}^{+\infty}\psi_tEE^*dx=\int_{-\infty}^{+\infty}[E_xE_x^*+(\alpha x+n)EE^*+\tfrac{1}{2}E_d(E+E^*)]dx\ . \quad (10)$$

Introducing the five time-dependent parameters x_0, q, η, a, and b, we use in the balance equations

$$E=\sqrt{2}(1-\dot{x}_0^2)^{1/2}q\eta\,\mathrm{sech}[\eta(x-x_0)]\exp[i(ax+b)]\ , \quad (11)$$

$$n=-2\eta^2q^2\mathrm{sech}^2[\eta(x-x_0)]\ , \quad (12)$$

$$u=-2\eta^2q^2\dot{x}_0\mathrm{sech}^2[\eta(x-x_0)]\ , \quad (13)$$

where the dot denotes derivative with respect to time. In this ansatz velocity, amplitudes, and width as well as the phase of the soliton are free parameters.

Introducing Eqs. (11), (12), and (13) into Eqs. (5), (6), and (8)–(10) we get the following five coupled ordinary differential equations:

$$\epsilon\frac{\partial}{\partial t}[q^2\eta(1-\dot{x}_0^2)]=-\frac{\pi}{2}E_d(1-\dot{x}_0^2)^{1/2}q\,\mathrm{sech}\left[\frac{a\pi}{2\eta}\right]\sin(b+ax_0)-2\Gamma(1-\dot{x}_0^2)\eta q^2\ , \quad (14)$$

$$\frac{\partial}{\partial t}[\epsilon a\eta q^2(1-\dot{x}_0^2)+\tfrac{4}{3}\eta^3q^4\dot{x}_0]=-\alpha(1-\dot{x}_0^2)\eta q^2-2\Gamma a\eta q^2(1-\dot{x}_0^2)\ , \quad (15)$$

$$\frac{\partial}{\partial t}\left[q^2\eta(1-\dot{x}_0^2)\left[\tfrac{1}{3}\eta^2+a^2-\tfrac{4}{3}q^2\eta^2+\alpha x_0\right]+\frac{\pi}{\sqrt{2}}E_dq(1-\dot{x}_0^2)^{1/2}\cos(b+ax_0)\mathrm{sech}\left[\frac{a\pi}{2\eta}\right]\right.$$
$$\left.+\tfrac{2}{3}\eta^3q^4+\tfrac{2}{3}\eta^3\dot{x}_0^2q^4\right]=2\Gamma(1-\dot{x}_0^2)\eta q^2(\dot{b}+\dot{a}x_0)\ , \quad (16)$$

$$(2a-\epsilon\dot{x}_0)\eta q^2(1-\dot{x}_0^2)=\frac{E_d\pi^2}{2\sqrt{2}}\frac{q}{\eta}(1-\dot{x}_0^2)^{1/2}\mathrm{sech}\left[\frac{a\pi}{2\eta}\right]\tanh\left[\frac{a\pi}{2\eta}\right]\cos(b+ax_0)\ , \quad (17)$$

$$-\epsilon(\dot{b}+\dot{a}x_0)=\tfrac{1}{3}\eta^2+a^2+\alpha x_0-\tfrac{4}{3}q^2\eta^2+\frac{E_d\pi}{2\sqrt{2}}[q\eta(1-\dot{x}_0^2)^{1/2}]^{-1}\mathrm{sech}\left[\frac{a\pi}{2\eta}\right]\cos(b+ax_0)\ . \quad (18)$$

We should note that the additional linear conservation laws

$$\frac{\partial}{\partial t}\int_{-\infty}^{+\infty}n\,dx=0 \quad (19)$$

and

$$\frac{\partial}{\partial t}\int_{-\infty}^{+\infty}u\,dx=0 \quad (20)$$

are not appropriate since one can not expect that they hold for the localized solitonlike solutions separately. They can be used to estimate the amount of radiation of ion-sound waves.[9]

We have not been able to solve these differential equations (14)–(18) analytically. Therefore, in Sec. III we treat some limiting cases and in Sec. IV we present numerical solutions of the initial-value problem.

III. THE UNDRIVEN SOLITON ($E_d=0$)

If we set $E_d=0$, the problem considerably simplifies. Physically, this situation occurs far from the

resonance, where the soliton moves in an inhomogeneous plasma only under the influence of damping. Then Eqs. (14)–(18) simplify to

$$\epsilon\frac{\partial}{\partial t}y=-2\Gamma y\ , \tag{21}$$

$$\frac{\partial}{\partial t}(\epsilon a y+\tfrac{4}{3}\eta^3 q^4\dot{x}_0)=-\alpha y-2\Gamma a y\ , \tag{22}$$

$$\frac{\partial}{\partial t}[y(\tfrac{1}{3}\eta^2+a^2-\tfrac{4}{3}q^2\eta^2+\alpha x_0)+\tfrac{2}{3}\eta^3(1+\dot{x}_0^2)q^4]=2\Gamma y(\dot{b}+\dot{a}x_0)\ , \tag{23}$$

$$(2a-\epsilon\dot{x}_0)y=0\ , \tag{24}$$

$$-\epsilon(\dot{b}+\dot{a}x_0)=\tfrac{1}{3}\eta^2+a^2+\alpha x_0-\tfrac{4}{3}q^2\eta^2\ , \tag{25}$$

where

$$y\equiv q^2\eta(1-\dot{x}_0^2)\ . \tag{26}$$

The rest of this section is devoted to a discussion of this set of equations.

A. Undamped inhomogeneous case ($\Gamma=0$)

Setting $\Gamma=0$, we obtain from Eqs. (21)–(24) [Eq. (25) will be an independent differential equation for b],

$$\frac{\epsilon^2}{2}q_0^2\eta_0\dot{x}_0+\tfrac{4}{3}q^4\eta^3\dot{x}_0=-\alpha q_0^2\eta_0 t\ , \tag{27}$$

$$\frac{\epsilon^2}{4}\eta_0 q_0^2\dot{x}_0^2-\eta_0^3 q_0^6(1-\dot{x}_0^2)^{-3}q^{-4}[(\tfrac{2}{3}q^4-\tfrac{1}{3})-(2q^2-\tfrac{1}{3})\dot{x}_0^2]+\eta_0^3 q_0^2(\tfrac{2}{3}q_0^4-\tfrac{1}{3})=-\alpha q_0^2\eta_0 x_0\ , \tag{28}$$

if we set $\eta(t=0)=\eta_0$, $\dot{x}_0(t=0)=0$, and $q(t=0)=q_0$.

Making use of the identity

$$\dot{x}_0\frac{d}{d\dot{x}_0}t=\frac{d}{d\dot{x}_0}x_0\ , \tag{29}$$

one finds after some algebra

$$\frac{dq^2}{d\dot{x}_0}(q^2-1)(\dot{x}_0^2-1)=-2\dot{x}_0 q^2(q^2-1)\ . \tag{30}$$

Thus, either

$$q^2\equiv 1 \tag{31}$$

or

$$q^2=q_0^2(1-\dot{x}_0^2)^{-1} \tag{32}$$

are the solutions. We disregard the first one, Eq. (31), since it is unstable. Any fluctuation will cause the solution (31) to flip to (32). Together with the formula

$$q^2\eta(1-\dot{x}_0^2)=\text{const}, \tag{33}$$

which follows from Eq. (21), we immediately get

$$\eta=\text{const}. \tag{34}$$

Setting, for simplicity, $q_0=1$, we get from Eq. (27) the time variation of the velocity $\dot{x}_0$ in the implicit form

$$t=-\frac{\epsilon^2}{2\alpha}\dot{x}_0-\frac{4\eta^2}{3\alpha}\frac{\dot{x}_0}{(1-\dot{x}_0^2)^2}\ . \tag{35}$$

The variation of b with the time follows from Eq. (25). Note that for large t, this equation can be approximated by

$$\dot{b}\simeq-\frac{\alpha}{\epsilon}x_0\ . \tag{36}$$

For completeness we present the solution for a,

$$a=\epsilon\dot{x}_0/2\ . \tag{37}$$

In Fig. 1, the relation (35) is depicted for the value

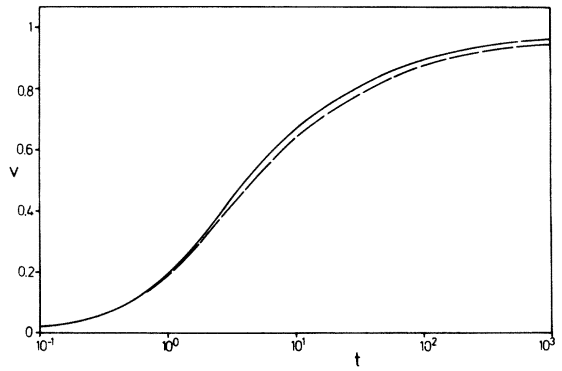

FIG. 1. Plot of the velocity v (in units c_s) vs time t (in units $\sqrt{3}/\omega_{pi}$) for $\alpha=0.003$ and $E_d=\Gamma=0$. Broken line depicts the result of Chukbar and Yankov, Ref. 6.

$\eta=0.1$. We clearly see that the maximum speed is $|\dot{x}_{0\max}|=1$, corresponding to c_s in dimensional units. This termination originates from the second term on the right-hand side of Eq. (35). Note that the first term is identical to the nonlinear Schrödinger result when the dynamic-plasma response is ignored. Because of ion inertia now the acceleration is much smaller than for the pure Schrödinger case.

Chukbar and Yankov[6] calculated the velocity of an undamped soliton in an inhomogenous plasma by a different (perturbative) method. If we rewrite their result in our notation, it reads

$$\ddot{x}_0=-\frac{2\alpha}{\epsilon^2}-\frac{8\eta^2}{3\epsilon^2}\ddot{x}_0(1+5\dot{x}_0^2)/(1-\dot{x}_0^2)^3 . \quad (38)$$

Integrating with respect to time and using the same initial conditions as before we obtain

$$t=-\frac{\epsilon^2}{2\alpha}\dot{x}_0-\frac{4\eta_0^2}{3\alpha}\left[\frac{3}{2}\frac{\dot{x}_0}{(1-\dot{x}_0^2)^2}-\frac{1}{4}\frac{\dot{x}_0}{1-\dot{x}_0^2}-\frac{1}{8}\ln\frac{1+\dot{x}_0}{1-\dot{x}_0}\right] . \quad (39)$$

We have also shown this result graphically in Fig. 1. Although the curve is not identical to our result, the two curves reasonably agree. This is an additional strong argument for the validity of the moment method used in this paper.

B. General aspects

We find the new result in our investigation that the width η^{-1} is constant. This mathematical result can be supported by physical arguments. The dynamical behavior of the width of the soliton is described by the following balance equation:

$$i\epsilon\frac{\partial}{\partial t}\int_{-\infty}^{+\infty}(x-x_0)^2EE^*dx=-4\int_{-\infty}^{+\infty}(x-x_0)EE_x^*dx-2\int_{-\infty}^{+\infty}EE^*dx+E_d\int_{-\infty}^{+\infty}(E^*-E)(x-x_0)^2dx-2i\Gamma\int_{-\infty}^{+\infty}(x-x_0)^2EE^*dx , \quad (40)$$

which follows from the perturbed Zakharov equations (3) and (4) after some straightforward algebra.

Introducing the ansatz (11)–(13) into Eqs. (40), we get

$$\epsilon\frac{\partial}{\partial t}\left[(1-\dot{x}_0^2)q^2\frac{\pi^2}{6\eta}\right]=-\frac{\Gamma\pi^2}{3\eta}q^2(1-\dot{x}_0^2) . \quad (41)$$

Combining Eqs. (21) and (41), one finds

$$y\frac{\partial}{\partial t}\eta^{-2}=0 . \quad (42)$$

Since $y\neq 0$ can be assumed without any loss of generality, we obtain $\eta=$const, which agrees with Eq. (34).

This result is interesting also in another respect. By adding the additional, in principle, independent equation (40) to the closed system of equations (21)–(25), we do not find a contradiction. This strongly supports the present method on physical grounds.

C. Acceleration because of damping

We now want to demonstrate another effect which does not occur when the dynamic-plasma response is neglected (as it is done in the cubic nonlinear Schrödinger case). For that we can even consider a homogeneous plasma ($\alpha=0$) but retain the phenomenological damping coefficient Γ. From the basic equations (21)–(26), with the initial condition $q_0=1$, we obtain the differential equation for x_0,

$$\ddot{x}_0\left[\frac{\epsilon^2}{2}+\frac{(\frac{4}{3}+4\dot{x}_0^2)\eta^2\exp(-2\Gamma t/\epsilon)(1-\dot{x}_{00}^2)}{(1-\dot{x}_0^2)^3}\right]=\frac{16}{3}\frac{\Gamma}{\epsilon}\eta^2\dot{x}_0(1-\dot{x}_0^2)^{-2}\exp(-2\Gamma t/\epsilon)(1-\dot{x}_{00}^2) , \quad (43)$$

where $\dot{x}_{00}$ is the initial velocity. Since Eq. (43) clearly shows

$$\ddot{x}_0\sim\Gamma\dot{x}_0 \quad (44)$$

we have proven the existence of acceleration because of damping. In Fig. 2 the solution of Eq. (43) is shown. We have also depicted the result of Chukbar and Yankov,[6] which, in our notation, reads ($\alpha=0$)

$$\ddot{x}_0\left[\frac{\epsilon^2}{2}+\tfrac{4}{3}\eta^2(1+5\dot{x}_0^2)(1-\dot{x}_0^2)^{-3}\right] =4\frac{\Gamma}{\epsilon}\eta^2\dot{x}_0(1-\dot{x}_0^2)^{-1}\,. \quad (45)$$

Again we find reasonably good agreement. We remark that such an acceleration due to damping does *not* follow from the Schrödinger description (when ion dynamics is neglected). This can be clearly seen from the perturbation treatment in Ref. 7.

We now generalize these findings to the *undriven* inhomogeneous case in the presence of damping. Then Eq. (43) has to be replaced by (for $\dot{x}_{00}=0$)

$$\ddot{x}_0\left[\frac{\epsilon^2}{2}+\frac{(\frac{4}{3}+4\dot{x}_0^2)\eta^2\exp(-2\Gamma t/\epsilon)}{(1-\dot{x}_0^2)^3}\right] =\frac{16}{3}\frac{\Gamma}{\epsilon}\eta^2\dot{x}_0(1-\dot{x}_0^2)^{-2}\exp(-2\Gamma t/\epsilon)-\alpha\,, \quad (46)$$

and Eq. (45) should read

$$\ddot{x}_0\left[\frac{\epsilon^2}{2}+\tfrac{4}{3}\eta^2(1+5\dot{x}_0^2)(1-\dot{x}_0^2)^{-3}\right] =4\frac{\Gamma}{\epsilon}\eta^2\dot{x}_0(1-\dot{x}_0^2)^{-1}-\alpha\,. \quad (47)$$

In Figs. 3 and 4, we have plotted the solutions of Eqs. (46) and (47). They show that damping enhances the velocity over that due to inhomogeneity. With increasing inhomogeneity strength and/or damping the velocity reaches sound velocity faster. Note that soon after a few characteristic ion times (ω_{pi}^{-1}) the sound velocity is reached for realistic α and Γ values. Then the velocity will not grow anymore. This has strong consequences for the position of the soliton. In contrast to the Schrödinger prediction, after a few characteristic ion times (ω_{pi}^{-1}) the soliton is still close to the resonance region ($x=0$). This will be important for the driven case which we will investigate now.

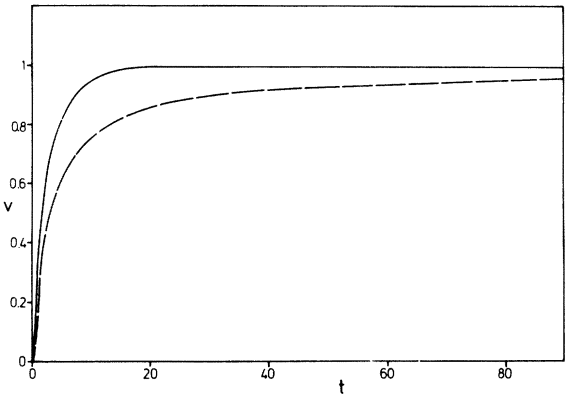

FIG. 3. Plot of the velocity v (in units c_s) vs time t (in units $\sqrt{3}/\omega_{pi}$) for the undriven case ($E_d=0$). Parameter values are $\alpha=0.003$ and $\Gamma=0.003$.

IV. THE DRIVEN SOLITON ($E_d\neq 0$)

We now return to the general case $E_d\neq 0$ as described by Eqs. (14) to (18). Before presenting the

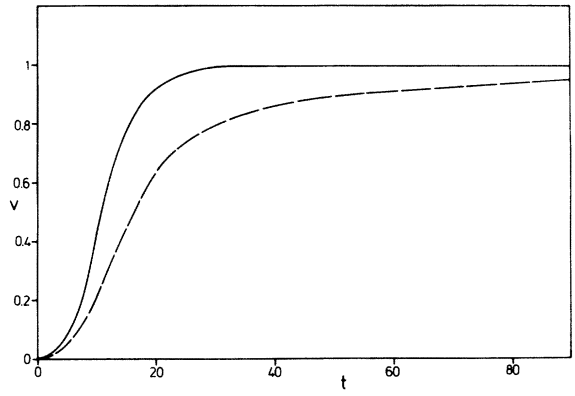

FIG. 2. Velocity v (in units c_s) vs time t (in units $\sqrt{3}/\omega_{pi}$) for $\Gamma=0.003$ and $E_d=\alpha=0$. Broken line depicts the result of Chukbar and Yankov, Ref. 6.

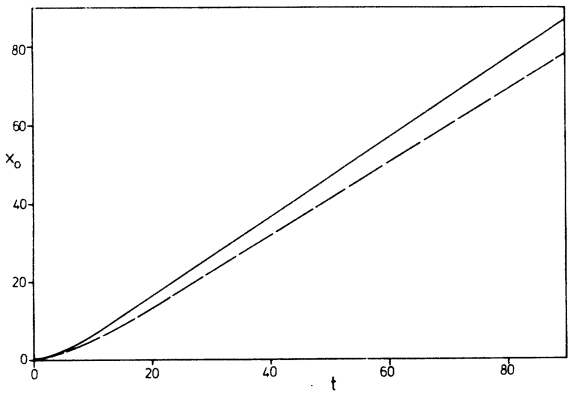

FIG. 4. Position x_0 (in units $\sqrt{3}\lambda_e$) vs time t (in units $\sqrt{3}/\omega_{pi}$) for the same parameters as in Fig. 3.

numerical solutions, we briefly discuss the damping decrement Γ. So far we set $\Gamma=\Gamma_0$ (constant) modeling some collisional damping. In order to also incorporate the Landau damping rate,

$$\nu=\left[\frac{\pi}{8}\right]^{1/2}\frac{\omega_{\rm pe}}{(\lambda_e k)^3}\exp\left[-\frac{3}{2}-\frac{\omega_{\rm pe}^2}{2k^2v_e^2}\right], \tag{48}$$

where v_e is the electron thermal velocity and k the wave number of the Langmuir wave, we proceed as follows. We use the dispersion relation

$$\omega^2\simeq\omega_{\rm pe}^2(1+3k^2\lambda_e^2), \tag{49}$$

to eliminate k. Then, we take into account the spatial inhomogeneity and the definition of the critical density to find

$$\frac{\omega}{\omega_{\rm pe}}\simeq\left[1+\frac{x}{L}\right]^{-1/2}. \tag{50}$$

Inserting Eqs. (49) and (50) into Eq. (48) and using the appropriate normalization, the result for Γ is

$$\Gamma=\left[\frac{27\pi}{8}\right]^{1/2}(1+\alpha x_0)^2(-\alpha x_0)^{3/2}\times\exp[\tfrac{3}{2}(\alpha x_0)^{-1}]+\Gamma_0, \tag{51}$$

where Γ_0 is the collisional damping rate. We therefore have a change of the damping rate with the soliton position x_0. This is physically plausible since the soliton is moving into the underdense region. For a fixed frequency of the carrier wave the wave number k thereby changes with position. This is exactly the meaning of Eq. (51) when seen in comparison with Eq. (48).

A. Numerical results

The numerical solutions show the following general behavior. The soliton formed will have its height increasing because of energy input due to the driver. The soliton saturates and becomes damped when it moves out of the resonance region due to acceleration in the density gradient and because of damping. The width of the soliton remains approximately constant. Large relaxation oscillations occur.

To demonstrate these results in more detail we show in Figs. 5–13, for different parameters E_d and α, the time dependence of three characteristic quantities: the velocity $v=|\dot{x}_0|$, the "energy"

$$W\equiv\frac{1}{4}\int|E|^2dx=q^2\eta(1-\dot{x}_0^2), \tag{52}$$

and the density depression

$$\delta n\equiv n_\infty-n_{\rm min}=2\eta^2r^2, \tag{53}$$

under the influence of collisional as well as Landau damping.

Let us first consider the velocity. The acceleration, and thereby the velocity of a soliton, is strongly influenced by ion mass effects. After an initial phase, the averaged velocity approaches the result for $E_d=0$. The velocity is always smaller than c_s. The bigger α and Γ, the larger is the acceleration.

In Figs. 6, 9, and 12 the relaxation and saturation behavior of the field energy is shown. We first observe that the field energy reaches a peak on the ion time scale. Saturation occurs in the undamped cases after many ion periods. If we compare with the curves for the Landau damped situation we recognize that Landau damping will change the results significantly; much less energy is contained in the solitons.

The density depression does not show large relaxation oscillations. As is seen from Figs. 7, 10, and 13 it slowly increases with time. Because of the coupling with the heavy ions, the response of the fluid density to radiation pressure oscillations is quite moderate.

The numerical results show that Landau damping becomes important after the soliton has traveled several Debye lengths away from the critical density ($x_0=0$). By inspection of formula (51) we can explain the drastic decrease of W in Fig. 9 (for $t\gtrsim400$) and Fig. 12 (for $t\geq80$) by the Landau damping. Before these times, the constant collisional damping Γ_0 is actually dominant. It causes the smooth damping of trapped radiation as seen in Fig. 6 for all times, in Fig. 9 for $t\leq400$, and in Fig. 12 for $t\leq80$. But when the soliton is moving into the underdense region, for a fixed frequency of the carrier wave the wave number increases with position. For $\alpha=0.02$ and $t\geq400$, as well as $\alpha=0.2$ and $t\geq80$, the Landau damping term overcomes the collisional damping rate Γ_0. Note that formula (51) tells us that the larger α is, the earlier Landau damping becomes important. Then, within short times the total damping rate increases significantly. Simultaneously, there is a drastic change in velocity as seen in Figs. 8 and 11. The reason for that acceleration because of damping has been discussed in Sec. III C. Finally, less trapped radiation results, via Eq. (4), in a smaller density cavity. When we solve for n, at least in the adiabatic approximation

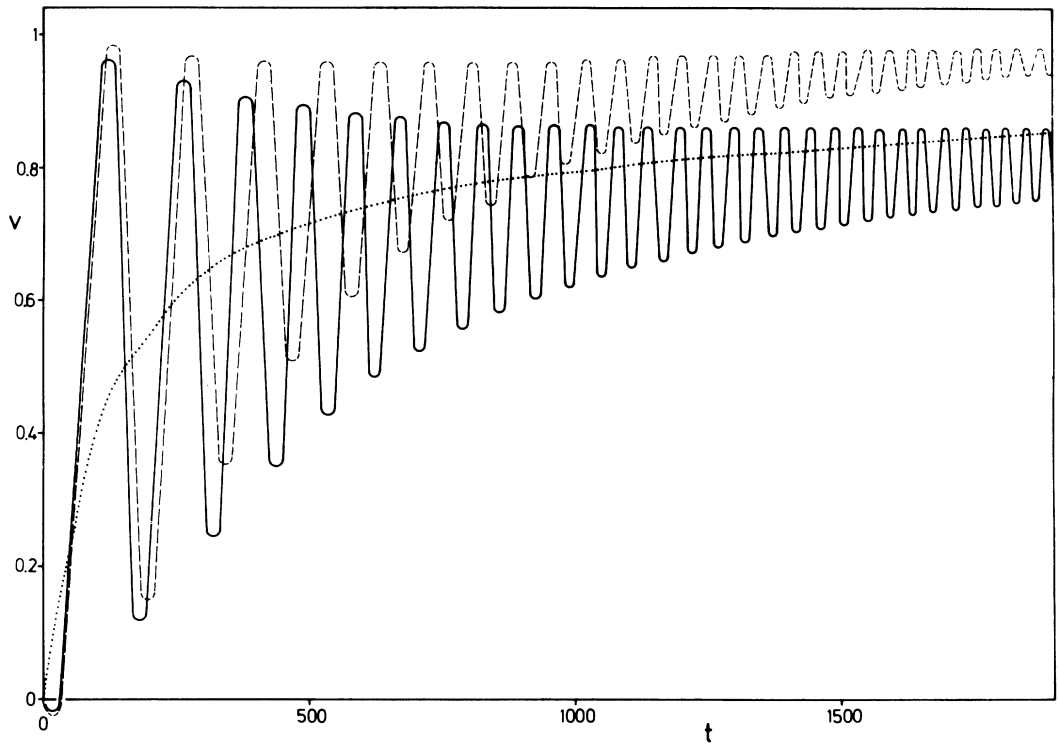

FIG. 5. Plot of the velocity v (in units c_s) vs time t (in units $2/\omega_{pe}$) for $E_d=0.0043$, $\alpha=0.003$. Solid line is without damping whereas the broken line depicts the result when Landau damping and collisional damping ($\Gamma_0=0.0005$) are included. Dotted line is the undriven result (see also Fig. 1).

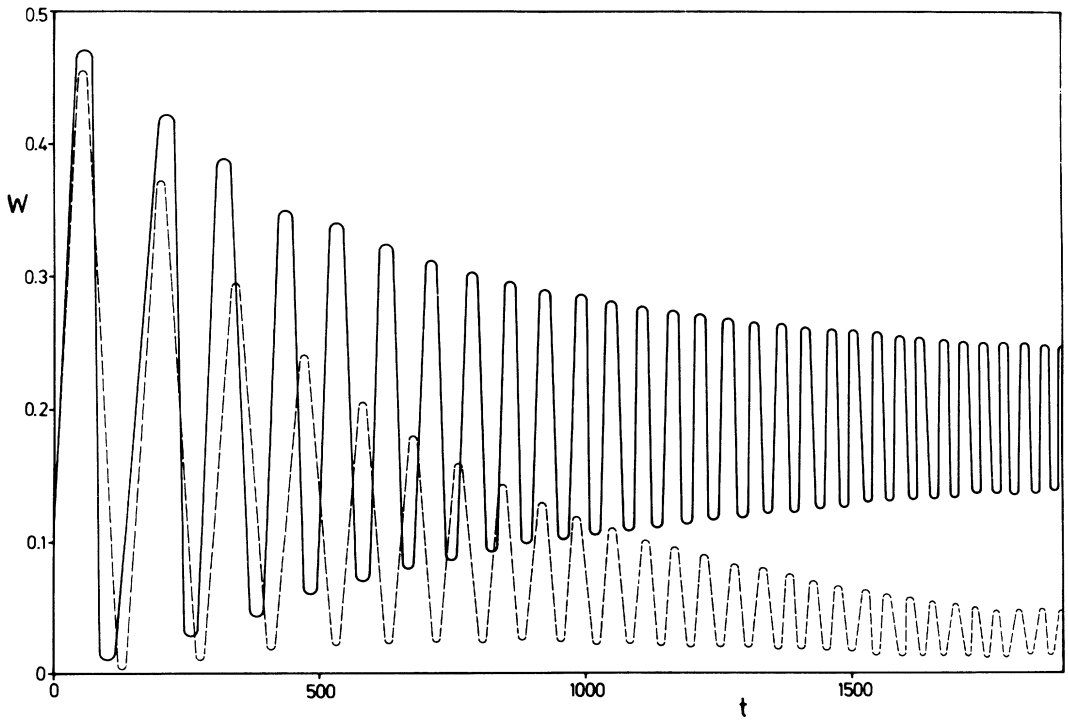

FIG. 6. Energy W vs t (in units $2/\omega_{pe}$) for the same parameters as in Fig. 5. Solid line is without damping whereas the broken line depicts the result when Landau and collisional damping are included.

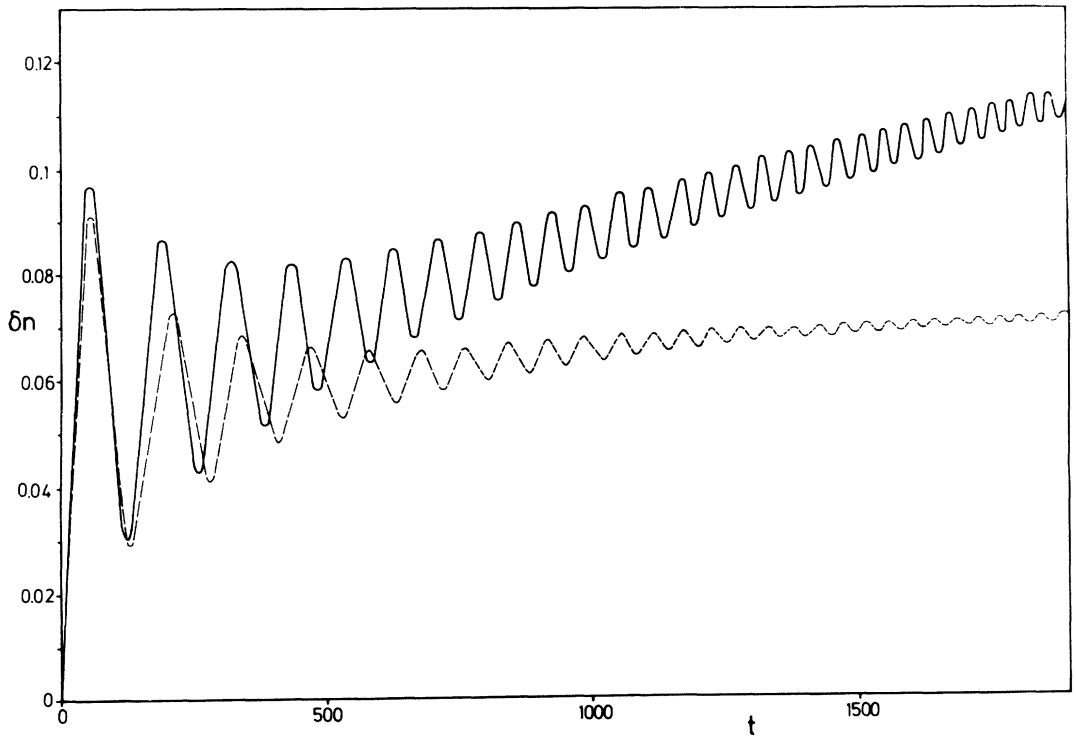

FIG. 7. Absolute maximum density depression δn (in units n_0) vs t (in units $2/\omega_{pe}$) for the same parameters as in Fig. 5. Solid line is without damping whereas the broken line depicts the result when Landau and collisional damping are included.

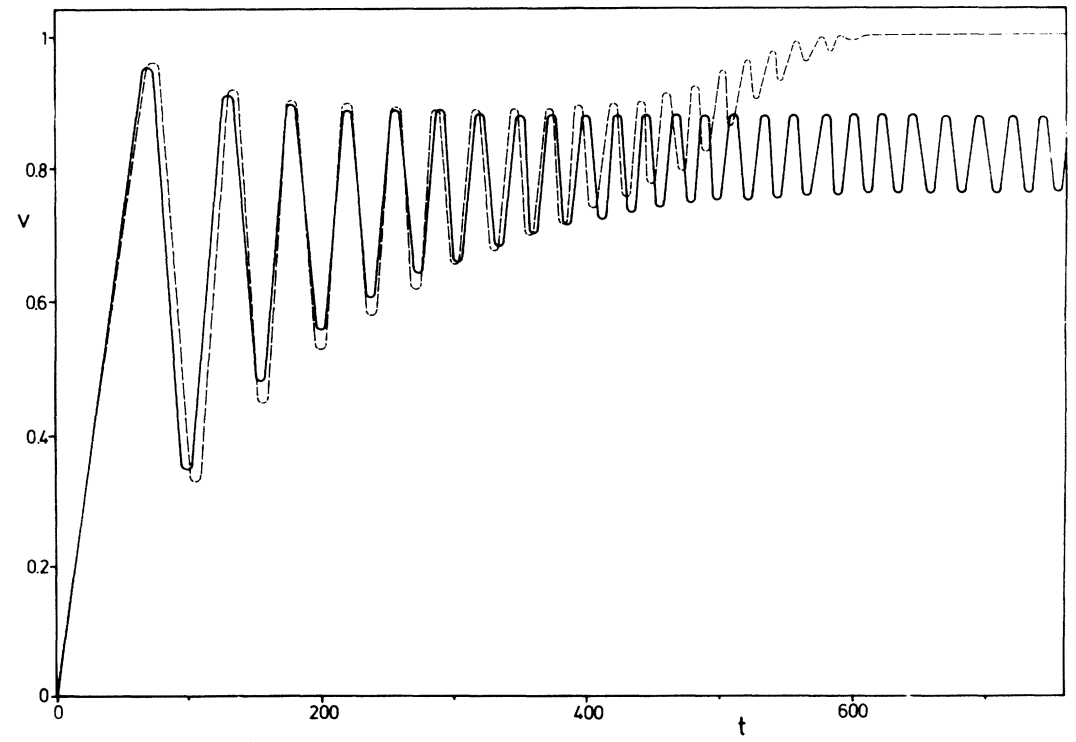

FIG. 8. Plot of velocity v vs time t for $E_d=0.014\,14$ and $\alpha=0.02$ (see also Fig. 5).

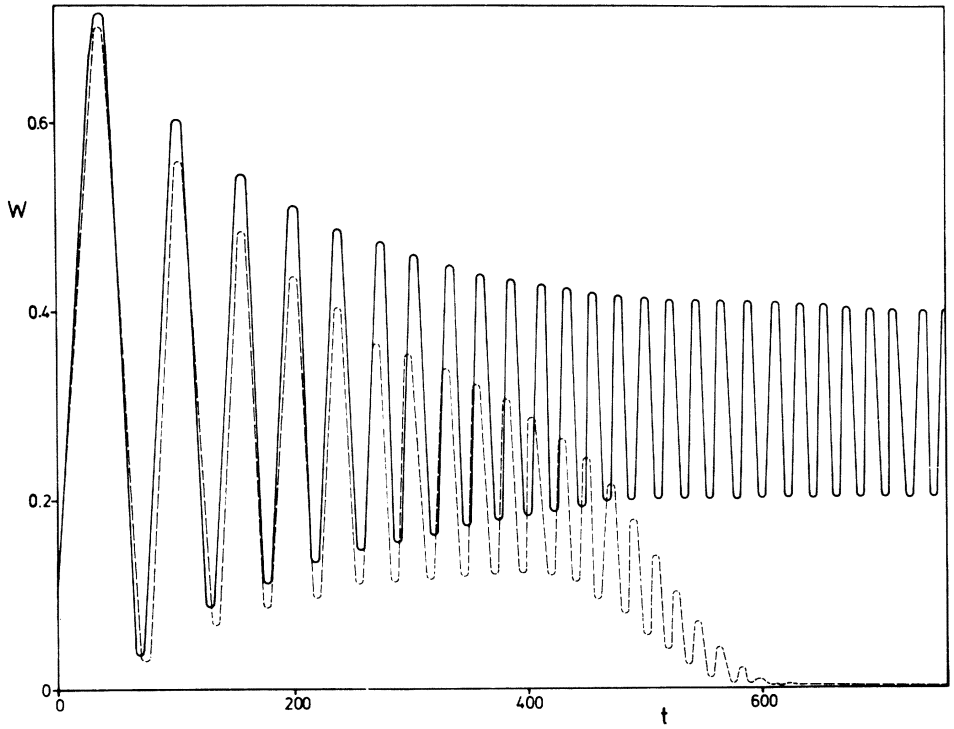

FIG. 9. W vs t for the same parameters as in Fig. 8 (see also Fig. 6).

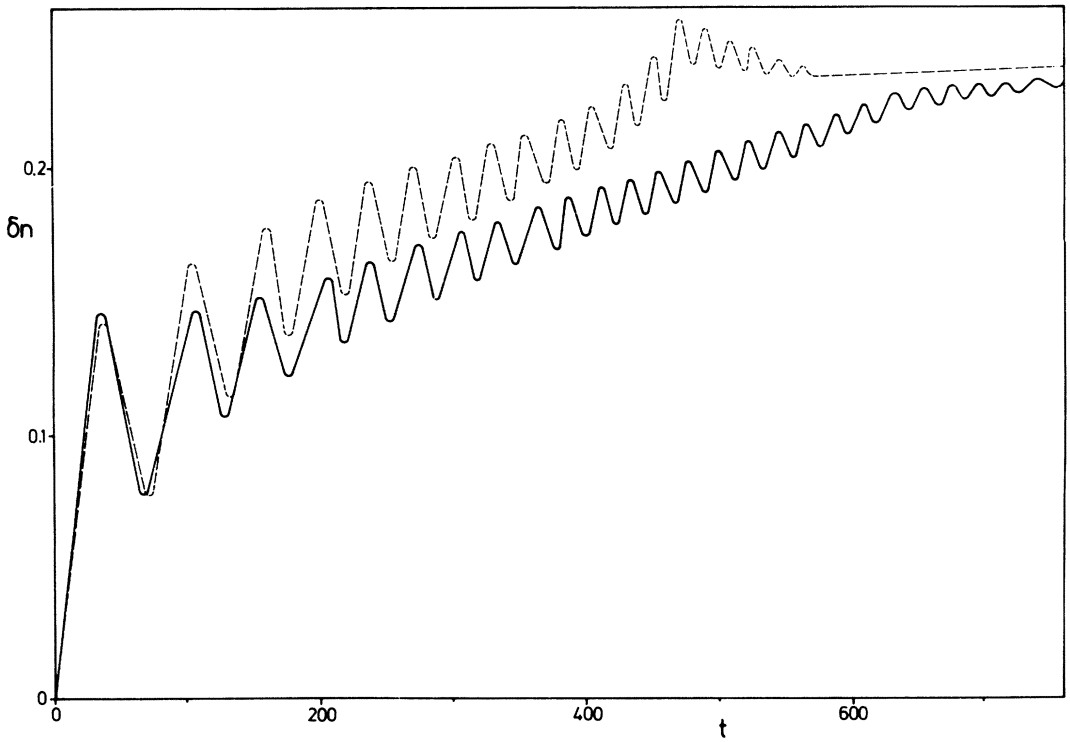

FIG. 10. δn vs t for the same parameters as in Fig. 8 (see also Fig. 7).

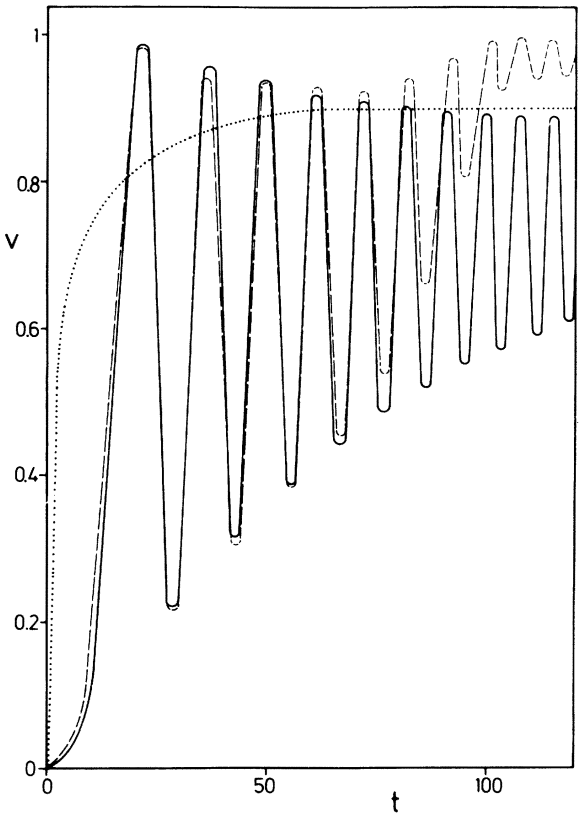

FIG. 11. v vs t for $E_d=0.1414$ and $\alpha=0.2$ (see also Fig. 5).

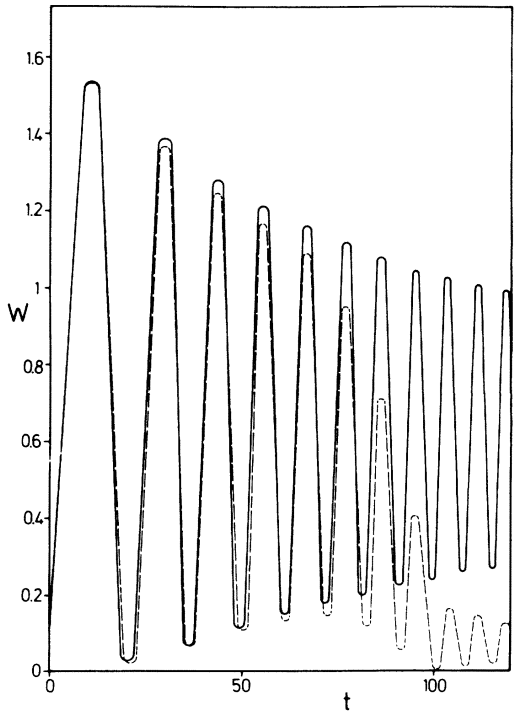

FIG. 12. W vs t for the same parameters as in Fig. 11 (see also Fig. 6).

the velocity also enters the picture. There are two competing effects: less trapped radiation (after damping) needs a smaller cavity but larger velocities make a larger cavity depth necessary. In Figs. 10 and 13 the resulting density depressions are presented where we can also see significant changes for $t \geq 400$ and $t \geq 80$, respectively. When W has been damped out, the ion equation (4) reads

$$\frac{\partial^2 n}{\partial t^2} - \frac{\partial^2 n}{\partial x^2} \simeq 0 , \tag{54}$$

indicating that the density depression can propagate unchanged in both directions. In our results we have shown only pulse propagation in one direction leading to $\delta n = \text{const}$ ($v \lesssim 1$ after sufficient damping) in Figs. 10 and 13.

B. Analytical estimates

Besides the already discussed (or obvious) effects of acceleration, energy growth, and damping, etc., the relaxation oscillations are the basic new features of the driven case. We now briefly estimate the fre-

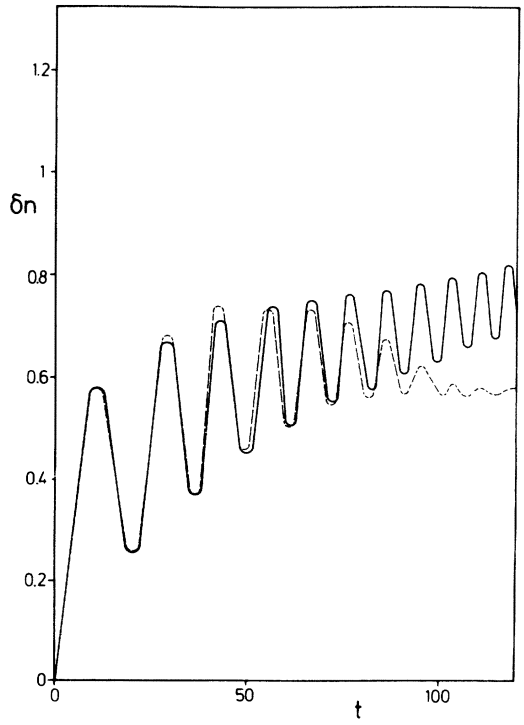

FIG. 13. δn vs t for the same parameters as in Fig. 11 (see also Fig. 7).

quency of these oscillations.

We have learned already that for $t \to \infty$, $|\dot{x}_0| \to 1$ and therefore

$$|x_0| \sim t \tag{55}$$

grows unlimited. Now, Eq. (18) can be approximated by

$$\frac{d}{dt}(b+ax_0) \simeq \frac{\alpha}{\epsilon} t \ , \tag{56}$$

where we have neglected all bounded terms as well as the term proportional to E_d. The latter neglection follows from

$$(1-\dot{x}_0^2)^{-1/2} \sim t^{1/4} \ll t \ .$$

We take the following solution of Eq. (56):

$$b+ax_0 \simeq -\frac{\pi}{2} + \frac{\alpha}{2\epsilon} t^2 \ . \tag{57}$$

Furthermore, for $\epsilon < \eta$ we have

$$\operatorname{sech}\left[\frac{a\pi}{2\eta}\right] \simeq 1 \tag{58}$$

and, in the undamped case, we get from Eq. (14)

$$\frac{dW}{dt} \simeq -\frac{\pi}{\epsilon\sqrt{2}} E_d \left[\frac{W}{\eta}\right]^{1/2} \sin\left[-\frac{\pi}{2} + \frac{\alpha}{2\epsilon} t^2\right] . \tag{59}$$

The solution of Eq. (59) is

$$W^{1/2} \simeq [W(t_0)]^{1/2} + \frac{\pi^{3/2} E_d}{2^{3/2} \alpha^{1/2} \epsilon^{1/2} \eta^{1/2}} \times \left[C\left[\frac{\alpha^{1/2} t}{\pi^{1/2} \epsilon^{1/2}}\right] - C\left[\frac{\alpha^{1/2} t_0}{\pi^{1/2} \epsilon^{1/2}}\right] \right] , \tag{60}$$

where $C(z)$ is the Fresnel integral. From (60) we see that the characteristic frequency at the nth maximum,

$$\omega_n = 2\pi/(\Delta t)_n \simeq \left[\frac{8\pi n \alpha}{\epsilon}\right]^{1/2} , \tag{61}$$

scales as $\alpha^{1/2}$.

Looking at the graphs (see Figs. 6, 9, and 12), we recognize that exactly with these frequencies a soliton is heavily pulsating. This phenomenon might be interpreted as a quasiperiodic generation of electric-field peaks and ion-density cavitons in the resonance region.

V. SUMMARY AND OUTLOOK

In this paper we have investigated the motion of Langmuir solitons in an inhomogeneous plasma under the influence of damping and driving terms. We have shown that ion inertia effects as well as damping effects are very important. Our numerical results show the energy transfer from the driver to the soliton and show its damping and acceleration. Analytical estimates for the relevant physical parameters are derived.

The method used is approximate and can describe only the gross behavior of the exact time-development. The emission of ion sound, the appearance of fast particles, and the generation of multisolitons and spikes need a more detailed investigation. Some of these problems are under investigation.

Another comment is in order: The Zakharov equations are only valid in the subsonic region and not when $|\dot{x}_0| - 1 \sim O(\epsilon)$. This puts an upper limit in time on the validity of our physical results. However, the moment method could be also applied to the near-sonic regime when a Korteweg–de Vries-like density response is taken into account.

Finally we mention that a related method has been successfully applied[15] to similar problems in molecular systems.

ACKNOWLEDGMENTS

We thank Padma Shukla for useful discussions and H. Kramer and D. Wiechert for numerical assistance. This work was partially supported by the Sonderforschungsbereich Plasmaphysik Bochum/Jülich, the Deutscher Akademischer Austauschdienst, and the ISRO/DFVLR exchange program.

[1] V. I. Karpman and E. M. Maslov, Zh. Eksp. Teor. Fiz. 73, 537 (1977) [Sov. Phys.—JETP 46, 281 (1977)].

[2] D. J. Kaup and A. C. Newell, Proc. R. Soc. London, Ser. A 361, 413 (1978).

[3] S. G. Thornhill and D. ter Haar, Phys. Rep. 43, 43 (1978).

[4] D. R. Nicholson and M. V. Goldman, Phys. Fluids 19, 1621 (1976).

[5]H. H. Chen and C. S. Liu, Phys. Rev. Lett. 37, 693 (1976).
[6]K. V. Chukbar and V. V. Yankov, Fiz. Plazmy 3, 1398 (1977) [Sov. J. Plasma Phys. 3, 780 (1977)].
[7]P. K. Shukla and K. H. Spatschek, J. Plasma Phys. 19, 387 (1978).
[8]D. R. Nicholson and M. V. Goldman, Phys. Fluids 21, 1766 (1978).
[9]A. Bondeson, Phys. Fluids 23, 746 (1980).
[10]L. H. Larsen, Phys. Fluids 23, 2359 (1980).
[11]E. W. Laedke and K. H. Spatschek, Phys. Rev. Lett. 45, 993 (1980).
[12]N. R. Pereira and L. Stenflo, Phys. Fluids 20, 1733 (1977).
[13]N. R. Pereira, Phys. Fluids 20, 1735 (1977).
[14]H. Sugai, H. Niki, and S. Takeda, Phys. Lett. 81A, 271 (1981).
[15]A. S. Davydov, Physica, D 3, 1 (1981).